

Tuning Electromagnetically Induced Transparency of Superconducting Metamaterial Analyzed with Equivalent Circuit Approach

Yonggang Zhang^{1, *}, Chun Li², and Xuecou Tu²

Abstract—We analyzed the effect of loss and coupling to EIT metamaterials using circuit approach, giving the effect of two parameters: coupling and loss on the resonant property of the EIT metamaterials. To verify the results of the circuit analysis, simulations and experiments were performed. The structures were fabricated with superconducting NbN and varied temperature to verify the effect of loss. The distances were adjusted to observe the effect of the coupling strength. The results of simulations and experiments were consistent with the circuit analysis.

1. INTRODUCTION

Electromagnetically induced transparency (EIT) is a quantum mechanical process observed in a certain three-level atomic system, which produces an extremely-narrow transparent window with low absorption and steep dispersion in an opaque medium [1–3]. The extreme dispersion of the EIT can reduce the group velocity of light by 7 orders in magnitude and store light temporally [4, 5]. Moreover, its narrow window can provide a well-defined frequency marker for precision measurement [6]. It provides a new way for realization of controlling the electromagnetic wave and has been widely used in optical manipulation. The research on EIT in atomic system encounters some problems. For example, it requires very low temperature, preparation of three-level system, and the operating frequency mainly in or near the visible region. The classical systems such as metamaterial for mimicking the phenomenon of EIT are adopted, and the working conditions and other requirements can be greatly reduced, very convenient for study relation between the operating frequency and various parameters. Moreover, its working frequency can be varied from microwave to visible light.

Metamaterials are subwavelength composites. Their electromagnetic properties are mainly determined by the internal and specific structures. They can manipulate the propagation of electromagnetic waves, leading to many fascinating electromagnetic phenomena, such as EIT [7–10], Fano resonance [11, 12], and chirality [13–15]. These new properties greatly extend the research scope of metamaterial and can find many new interesting applications in polarization control, giant optical activity, asymmetric EM wave propagation, quantum information process, and biosensors.

Metamaterial has many fascinating physical properties, but large loss is the main problem hindering its practical application, so low loss superconducting metamaterial increasingly attracts the attention of researchers [16]. The conductivity of superconductor can be varied by the excitation such as magnetic field, laser, or temperature. It provides a new way for tuning properties of metamaterial.

In 2005, Ricci et al. produced superconducting metamaterials at microwave frequency using superconducting Nb and achieved negative refractive index [17]. They proved that the physical

Received 21 December 2019, Accepted 25 March 2020, Scheduled 3 April 2020

* Corresponding author: Yonggang Zhang (ygzhang2000@163.com).

¹ School of Electrical and Information Engineering, Anhui University of Science and Technology, Huainan, Anhui 232001, China.

² Research Institute of Superconductor Electronics (RISE), School of Electronic Science and Engineering, Nanjing University, Nanjing 210093, China.

properties of superconducting metamaterial could be tuned by temperature and magnetic field [18]. Superconductor has very low ohmic loss at terahertz band, suitable for fabrication of terahertz metamaterial. Gu et al. prepared the THz metamaterial using superconducting YBCO and found that its transmission spectrum could change with temperature in superconducting state [19]. NbN is a low temperature superconductor. The metamaterial fabricated by NbN can maintain low loss at a higher frequency. NbN metamaterial has a characteristic of temperature tuning because its complex conductivity could vary with temperature. Wu et al. have fabricated NbN metamaterial at terahertz frequency and achieved temperature control [20–23]. The results show that NbN metamaterial exhibits good performance of tuning.

Here, we extend the equivalent circuit model to explore the resonance property of EIT metamaterial. In the proposed model, each bright and dark resonator in a unit cell is described as a resonant circuit with a resistor R , an inductor L , and a capacitor C in series. The whole unit cell is equivalent to two resonance circuits coupled through the coupling capacitance. Through such an equivalent circuit approach, we are able to analyze the resonance properties of the EIT metamaterial rigorously. In addition, the property of the EIT metamaterial can be easily tuned by changing the circuit parameters. We also carried out simulation of an EIT metamaterial at terahertz frequency and compared it with the one from the equivalent circuit model. Finally, experiment with superconducting NbN structure was carried out to verify the circuit analysis. The results of simulation and experiments are consistent with the circuit analysis.

2. CIRCUIT ANALYZE

To study the resonant property of EIT metamaterial, we consider a typical EIT structure as shown in Fig. 1. Each unit cell consists of two spatially separated resonators. The straight metal strip is a bright resonator coupled to the incident THz wave directly. The dark resonator is a double-gap split ring resonator (DSRR). The incident electromagnetic wave is normal to the plane of the metamaterial (z -axis) with polarization along y -direction. Fig. 2 shows the equivalent circuit model for the EIT metamaterial of the structure.

In circuit model, each resonator is a resonance structure which can be described as an RLC resonance circuit [24, 25]. The subscript 1 following the parameters RLC represents the bright resonator (loop 1), and subscript 2 represents the dark resonator (loop 2). The whole unit cell is equivalent to two resonance circuits coupled through the capacitance C . If the resonant frequencies of two resonators are set equal, we obtain $L_1C_1 = L_2C_2$. The circuit current directions are set positive when its direction is

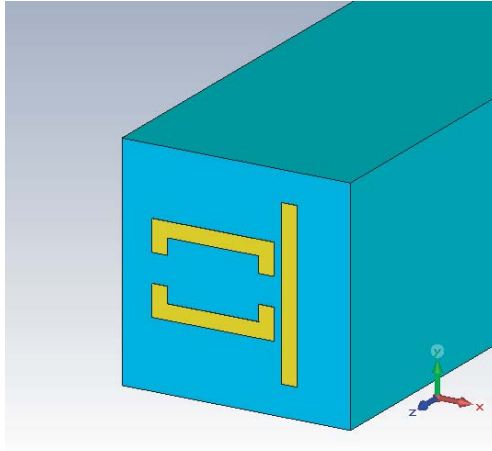


Figure 1. The Unit cell of EIT metamaterial. The dimension of periodic structure is $120\ \mu\text{m} \times 120\ \mu\text{m}$, where bright resonator with the dimensions of $8\ \mu\text{m} \times 88\ \mu\text{m}$, dark resonator with the dimensions of $64\ \mu\text{m} \times 48\ \mu\text{m}$. The width of metal strip of dark resonator is $8\ \mu\text{m}$. The gaps of the dark resonator are $15\ \mu\text{m}$. Thickness of resonators are $0.2\ \mu\text{m}$. The substrate is $1000\ \mu\text{m}$ -thick MgO.

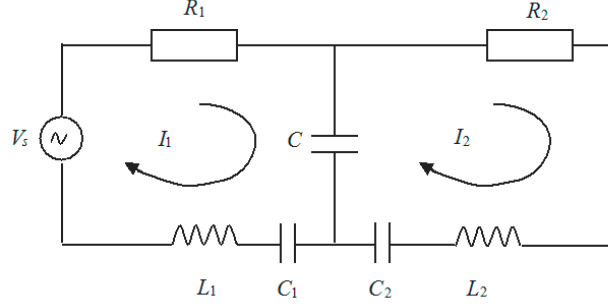


Figure 2. Equivalent circuit for the EIT metamaterial.

clockwise. Frequency adjustable power V_s represents detecting field, namely the incident electromagnetic waves.

According to relationships between the two-oscillators model and circuit model [25–28], the circuit equations for EIT metamaterial based on Kirchhoff's law are as follows:

$$\begin{aligned} \dot{V}_s &= R_1 \dot{I}_1 + j\omega L_1 \dot{I}_1 + \frac{1}{j\omega C_1} \dot{I}_1 - \frac{1}{j\omega C} \dot{I}_2 \\ 0 &= R_2 \dot{I}_2 + j\omega L_2 \dot{I}_2 + \frac{1}{j\omega C_2} \dot{I}_2 - \frac{1}{j\omega C} \dot{I}_1 \end{aligned} \quad (1)$$

Here, $I_1(t) = \dot{q}_1(t)$; $I_2(t) = \dot{q}_2(t)$, where $q_1(t)$, $q_2(t)$ represent the charges in loop 1 and loop 2 respectively. From Eq. (1), we obtain:

$$\dot{V}_s = \left(R_1 + j\omega L_1 + \frac{1}{j\omega C_1} \right) \dot{I}_1 - \frac{\left(\frac{1}{j\omega C} \right)^2}{R_2 + j\omega L_2 + \frac{1}{j\omega C_2}} \dot{I}_2 \quad (2)$$

Assuming that Z_1 is the impedance of loop 1, we obtain: $Z_1 = \frac{\dot{V}_s}{\dot{I}_1}$. Assume $\xi_1 = (\omega L_1 - \frac{1}{\omega C_1})$; $\xi_2 = (\omega L_2 - \frac{1}{\omega C_2})$; $\eta^2 = (\frac{1}{\omega C})^2$. Z_1 can be written as follows:

$$Z_1 = (R_1 + j\xi_1) + \frac{\eta^2}{(R_2 + j\xi_2)} \quad (3)$$

$$Z_1 = \frac{1}{(R_2^2 + \xi_2^2)} \left[(R_1 R_2^2 + R_1 \xi_2^2 + R_2 \eta^2) + j\xi_1 \left(R_2^2 + \xi_2^2 - \frac{\xi_2}{\xi_1} \eta^2 \right) \right] \quad (4)$$

If loop 1 is in resonant state, the imaginary part of Z_1 would equal to zero, which yields:

$$\xi_1 \left(R_2^2 + \xi_2^2 - \frac{\xi_2}{\xi_1} \eta^2 \right) = 0 \quad (5)$$

The solutions of Eq. (5) are quite different depending on the values of R_2 and η if the other circuit parameters (L_1 , L_2 , C_1 , C_2) are constant. When $\frac{\eta^2}{R_2^2} < \frac{L_1}{L_2}$, one of the solutions of Eq. (5) is $\xi_1 = 0$, giving the resonance frequency equal to $\omega = \sqrt{1/L_1 C_1}$. The other solution requires $\xi_2 < 0$, which is purely imaginary and is meaningless in physics. When $\frac{\eta^2}{R_2^2} = \frac{L_1}{L_2}$, Eq. (5) has only one solution, which is $\xi_1 = 0$ or $\xi_2 = 0$, giving the resonance frequency the same as the previous occasion, equal to $\omega = \sqrt{\frac{1}{L_1 C_1}} = \sqrt{\frac{1}{L_2 C_2}}$. However, when $\frac{\eta^2}{R_2^2} > \frac{L_1}{L_2}$, there exist three solutions of Eq. (5). These solutions are $\xi_2 = \pm \sqrt{\frac{L_2}{L_1} \eta^2 - R_2^2}$ and $\xi_1 = 0$. However, $\xi_1 = 0$ corresponds to the minimum of I_2 , and it does not correspond to the resonant case. There exist two resonance frequencies, which are determined from the solutions of $\xi_2 = \pm \sqrt{\frac{L_2}{L_1} \eta^2 - R_2^2}$.

From the previous analysis, we know that there exists only one resonant frequency for $\frac{\eta^2}{R_2^2} \leq \frac{L_1}{L_2}$, but two resonance frequencies for $\frac{\eta^2}{R_2^2} > \frac{L_1}{L_2}$. Only one resonant dip obtained in transmission spectra indicates that there is no EIT-like spectral response. If there are two resonance dips in the transmission spectra, the EIT-like phenomenon therefore appears.

Through the equivalent circuit approach, we are able to analyze the resonance properties of the EIT metamaterial rigorously, providing simple and innovative ways to understand the underlying physical mechanism. In addition, the parameters of EIT metamaterial can be easily tuned by changing the resistance, capacitance, and coupling capacitance. From the previous analysis, there are two ways for changing properties of the EIT metamaterial. One is changing coupling strength between two resonators, which can be realized by changing the distance between resonators. The other is changing the loss of the structure. The loss of metamaterial includes radiation loss and ohmic loss. Ohmic loss can be controlled by changing the conductivity of metal [21–23]. For example, we can change the conductivity of the superconductor through temperature varying.

3. SIMULATION AND EXPERIMENT

To verify our equivalent circuit analysis, the simulated and measured transmission responses of the EIT metamaterial were carried out. The structures were formed in NbN films deposited on 1000- μm -thick MgO substrates ($\langle 100 \rangle$ orientation). The NbN films typically have a critical temperature (T_c) of 15.8 K.

Firstly, we calculated the transmission spectrums at different distances (d) between resonators for analyzing the effect of the coupling strength to EIT as shown in Fig. 3. When $d = 2 \mu\text{m}$ as shown in Fig. 3(a), the EIT metamaterial has the largest coupling strength because small distance makes coupling strong. Although R_2^2 varies with the temperature from 8 k to 18 k, η^2 gets maximum for all d , which makes the values of $\frac{\eta^2}{R_2^2}$ greater than $\frac{L_1}{L_2}$, and the EIT phenomenon exists for all temperature. Because the loss varies with temperature, the difference of two resonant frequencies and the quality factors (Q) will change with temperature as shown in Fig. 3(a).

When distance increases under constant temperature, the coupling strength (η^2) will decrease accordingly, but the ohmic loss of the metamaterial is nearly constant. Therefore, the changing direction of $\frac{\eta^2}{R_2^2}$ will also decrease with the increase of distance accordingly. It will vary from greater than $\frac{L_1}{L_2}$ towards equal to $\frac{L_1}{L_2}$, and smaller than $\frac{L_1}{L_2}$ at last. As shown in Fig. 3, with increase of d , the coupling effect becomes weaker, and the transmittance peak gradually decreases. For distance varying from 2 μm to 18 μm , there are two resonance dips in transmission spectra, which subsequently merge into one. As shown in Fig. 3(c), only one resonant frequency is obtained when temperature is 15 k. Continually increasing d , more and more system configurations satisfy $\frac{\eta^2}{R_2^2} < \frac{L_1}{L_2}$. This behavior can be attributed to the change of η^2 as d varies. As our circuit model predicts, the transmission spectra are dependent on the d value.

Another way for changing η^2 is letting metal conductivity have different values. Since R originates from ohmic and radiation loss, different metal conductivities mean different ohmic losses, i.e., different R . If raising the temperature of NbN from 8 k to 18 k at constant distance, the loss of the system will increase, and η^2 is nearly constant. The value of $\frac{\eta^2}{R_2^2}$ will decrease accordingly. The changing direction of $\frac{\eta^2}{R_2^2}$ also varies from greater than $\frac{L_1}{L_2}$ towards equal to $\frac{L_1}{L_2}$, and smaller than $\frac{L_1}{L_2}$ at last. For temperature rising from 8 k to 18 k, there are also two resonance dips in the transmission spectra, which subsequently merge into one as typically shown in Fig. 3(c). This behavior can be attributed to the change of R with varying temperature as predicted by our circuit model.

In the process of two resonance dips merging into one, the phenomenon of EIT is gradually weakened, until the disappearance. The result is consistent with the circuit model analysis.

We present the resonant frequency dependence on parameters of η^2 and R together as shown in Fig. 4. The abscissa represents the distance between resonators, and the ordinate represents frequency. From Fig. 4, we can see clearly that these two factors together determine the resonant property of EIT

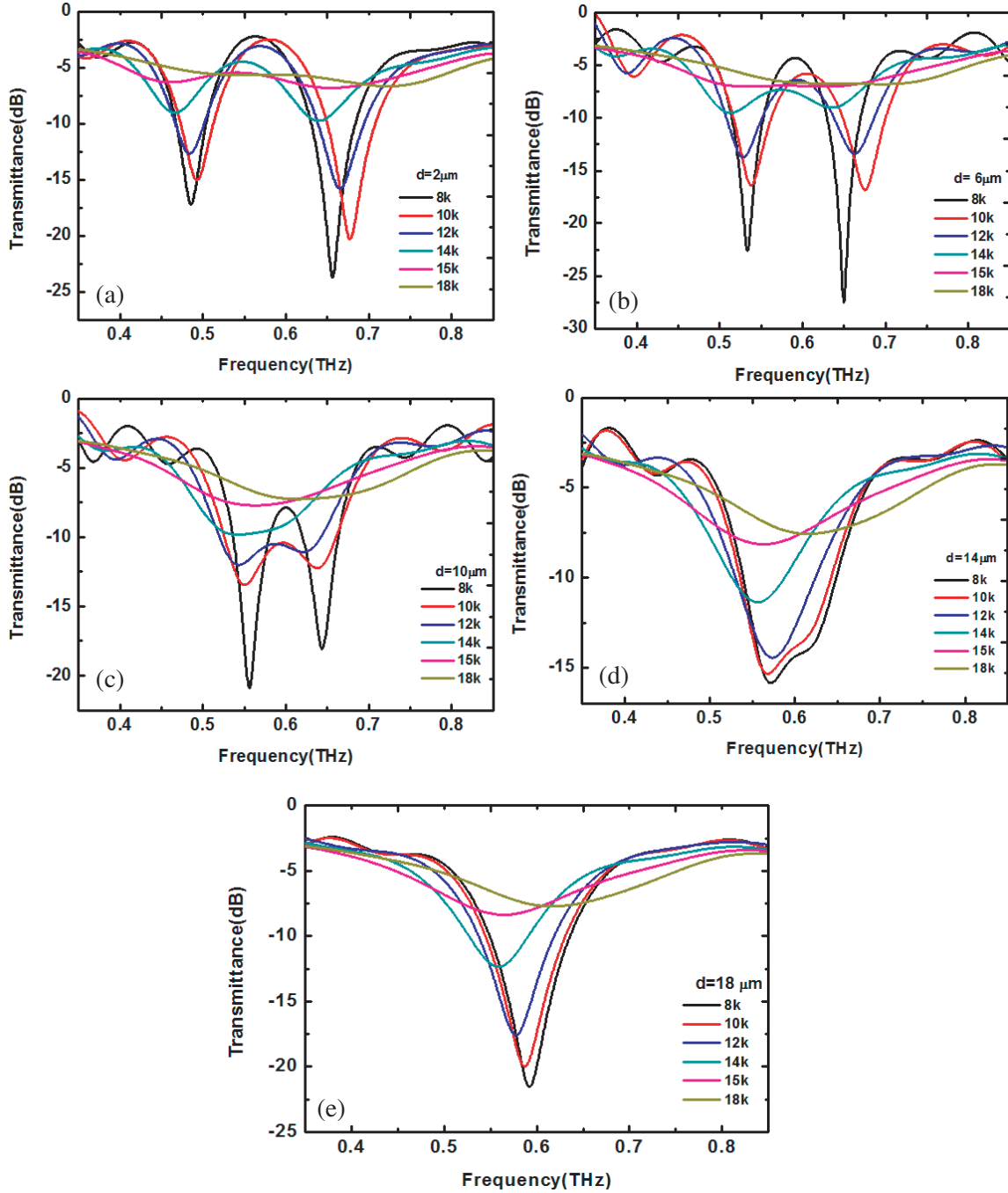


Figure 3. Simulated transmission spectra of the EIT NbN metamaterials.

metamaterial. When $d = 2 \mu\text{m}$, due to strong coupling, $\frac{\eta^2}{R_2^2}$ are greater than $\frac{L_1}{L_2}$ under all temperatures from 8k to 18k. The system has two resonant frequencies, and the transparency peak is observed. When $d = 8 \mu\text{m}$ at 15k, $\frac{\eta^2}{R_2^2}$ is reduced to smaller than $\frac{L_1}{L_2}$; the structure has only one resonant frequency; and EIT phenomenon disappears. Then continue to increase d , the structure cannot show the EIT phenomenon any more. When $d = 16 \mu\text{m}$, all structures cannot show EIT phenomenon at any temperature.

Finally, we fabricated a series of terahertz EIT samples using superconducting NbN. By temperature

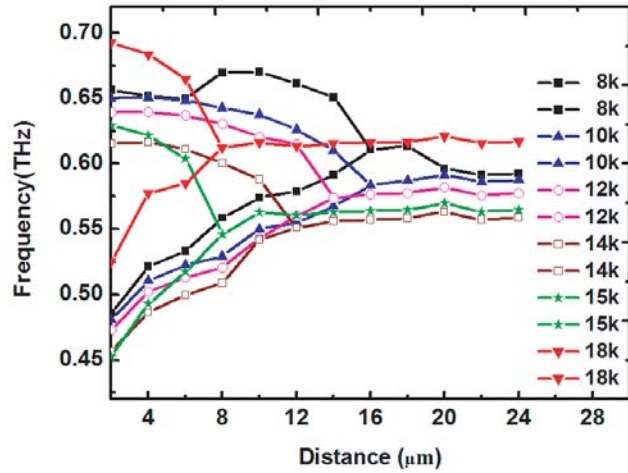


Figure 4. Resonant frequencies varied with the distance and temperature.

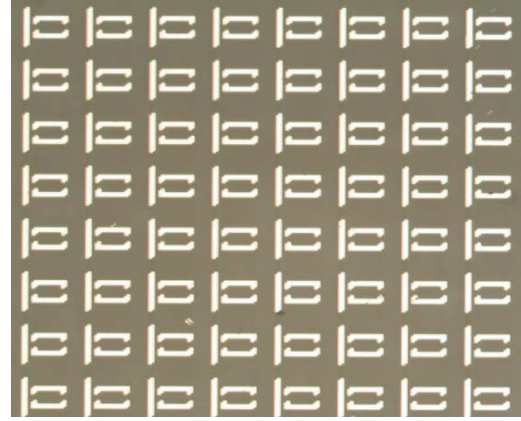
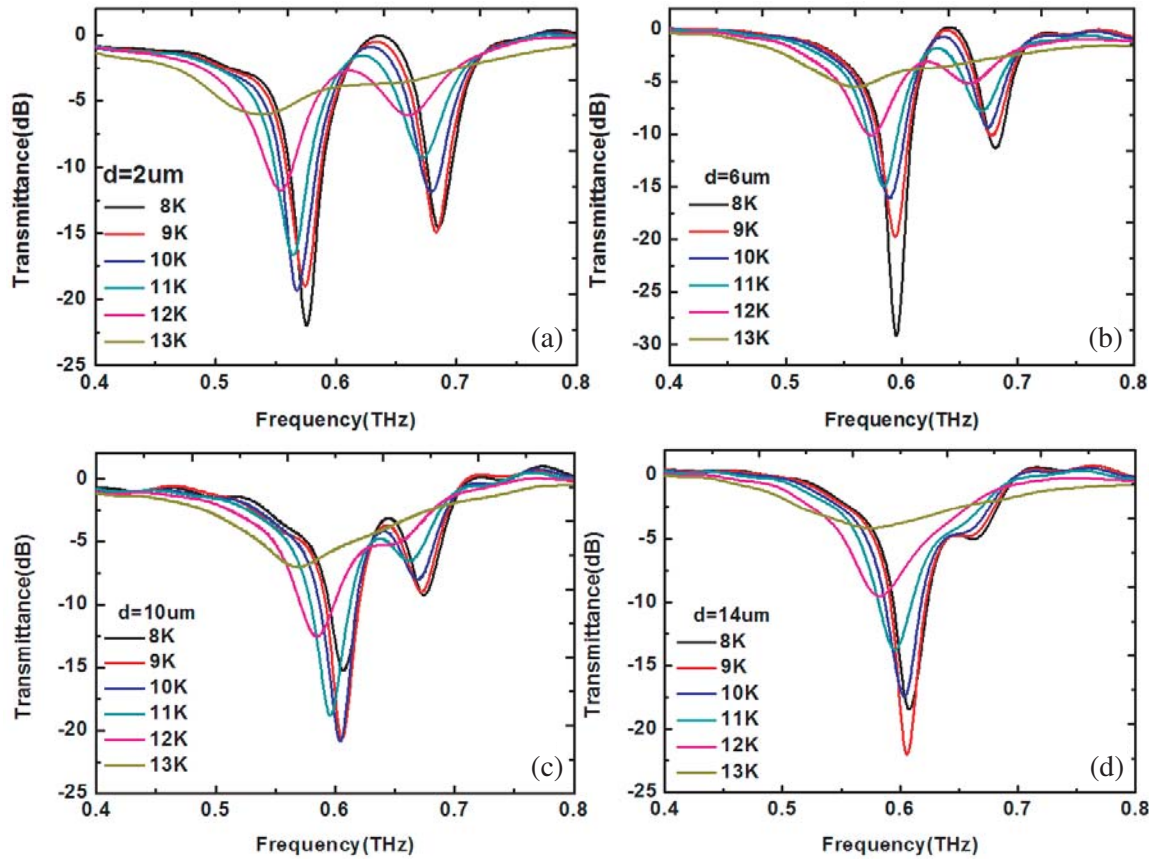


Figure 5. Microscopic images for the fabricated EIT metamaterials ($d = 6 \mu\text{m}$).

tuning and structural changing, we carried out measurement to verify the conclusion of circuit model and simulation. We characterized the samples by terahertz time-domain spectroscopy (THz-TDS) for transmission spectrum of superconducting THz metamaterial. The conductivity of the NbN was varied by the temperature control near the T_c of NbN using a liquid helium cryogenic system.

The dimensions of the samples are consistent with the simulation. NbN was fabricated on the MgO substrate. Experimental samples were prepared in five different distances varying from $2 \mu\text{m}$ to $18 \mu\text{m}$ with the interval of $4 \mu\text{m}$. One of the samples is shown in Fig. 5. The resulting transmission spectrums



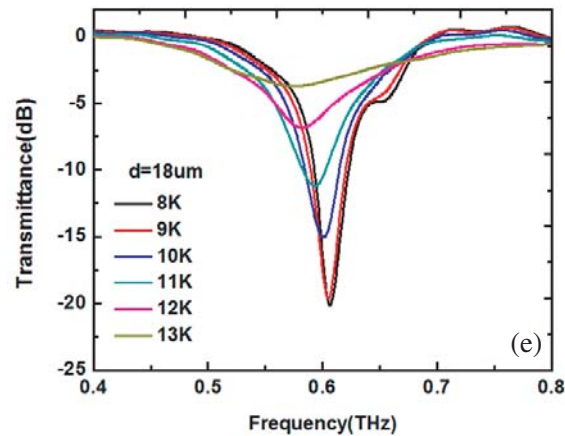


Figure 6. Measured transmission responses for different d and different temperature.

are shown in Fig. 6.

From Fig. 3 and Fig. 4, we can see that the measurement and simulation are consistent with the circuit model analysis. A trivial difference between measurement and simulation is the transmission responses in simulation which are better than the experimental results. This may be attributed to some minor defects in structure as well as curved surfaces, which result in the addition losses and other differences.

4. CONCLUSION

In this paper, we analyze the effect of resistance and coupling strength to EIT of metamaterials using circuit model. Through the circuit analysis, it can be known that whether the system produces EIT phenomenon depends on the comparison between coupling and loss. From circuit analysis, there are two ways to tune the EIT resonance: one is changing the coupling strength between resonators, which can be achieved by adjusting the distance between two resonators. The other method is fabrication of a superconducting NbN structure, under the regulation of low temperature to change the conductivity of the superconducting for achieving tuning loss of the structure.

We performed simulation and experiment to validate the results of the circuit analysis. The results of simulation and experiment are consistent with the circuit analysis. The measurement and simulation prove that preceding circuit model analysis is correct. The circuit analysis provides a simple and effective way to understand the coupling of the metamaterial and gives guidance for the analysis and design of metamaterial.

ACKNOWLEDGMENT

This work is supported by the Key Programs of Natural Science Foundation of Higher Education Institution of Anhui Province, China (KJ2016A195); Programs of Doctor Foundation of AnHui University of Science and Technology (11679).

REFERENCES

1. Harris, S. E., "Electromagnetically induced transparency," *Physics Today*, Vol. 50, 36–42, 1997.
2. Fleischhauer, M., A. Imamoglu, and J. P. Marangos, "Electromagnetically induced transparency: Optics in coherent media," *Review of Modern Physics*, Vol. 77, 633–673, 2005.
3. You, J. Q. and F. Nori, "Atomic physics and quantum optics using superconducting circuits," *Nature*, Vol. 474, 589–597, 2011.

4. Hau, L. V., S. E. Harris, Z. Dutton, and C. H. Behroozi, "Light speed reduction to 17 metres per second in an ultracold atomic gas," *Nature*, Vol. 397, 594–598, 1999.
5. Phillips, D. F., A. Fleischhauer, A. Mair, R. L. Walsworth, and M. D. Lukin, "Storage of light in atomic vapor," *Physical Review Letters*, Vol. 86, 783–786, 2001.
6. Boyd, R. W. and D. J. Gauthier, "Photonics: transparency on an optical chip," *Nature*, Vol. 441, No. 7094, 701–702, 2006.
7. Fedotov, V. A., M. Rose, S. L. Prosvirnin, N. Papasimakis, and N. I. Zheludev, "Sharp trapped-mode resonances in planar metamaterials with a broken structural symmetry," *Physical Review Letters*, Vol. 99, 147401, 2007.
8. Papasimakis, N., V. A. Fedotov, N. I. Zheludev, and S. L. Prosvirnin, "Metamaterial analog of electromagnetically induced transparency," *Physical Review Letters*, Vol. 101, No. 4, 253903, 2008.
9. Shao, J., P. Chen, R. X. Wu, et al., "Analogue of electromagnetically induced transparency by doubly degenerate modes in a U-shaped metamaterial," *Appl. Phys. Lett.*, Vol. 102, 034106, 2013.
10. Zhang, S., Dentcho A. Genov, Y. Wang, M. Liu, and X. Zhang, "Plasmon-induced transparency in metamaterials," *Physical Review Letters*, Vol. 101, 047401, 2008.
11. Yanchuk, B. L., N. I. Zheludev, N. J. Halas, et al., "The Fano resonance in plasmonic nanostructures and metamaterials," *Nat. Mater.*, Vol. 9, 707–715, 2010.
12. Cao, W., R. Singh, I. A. Naib, et al., "Low-loss ultra-high-Q dark mode plasmonic Fano metamaterials," *Opt. Lett.*, Vol. 37, 3366–3368, 2012.
13. Zhu, L., L. Dong, J. Guo, et al., "Polarization-independent transparent effect in windmill-like metasurface," *Journal of Physics D: Applied Physics*, Vol. 51, No. 26, 2018.
14. Zhu, L., X. Zhao, et al., "Dual-band polarization convertor based on electromagnetically induced transparency (EIT) effect in all-dielectric metamaterial," *Optics Express*, Vol. 27, 12163, 2019.
15. Liu, N., H. Liu, S. N. Zhu, et al., "Stereometamaterials," *Nat. Photon*, Vol. 3, 157–162, 2009.
16. Anlage, S. M., "The physics and applications of superconducting metamaterials," *Journal of Optics*, Vol. 13, 024001, 2011.
17. Ricci, M., N. Orloff, and S. M. Anlage, "Superconducting metamaterials," *Applied Physics Letters*, Vol. 87, 034102, 2005.
18. Ricci, M. C., H. Xu, R. Prozorov, A. P. Zhuravel, A. V. Ustinov, and S. M. Anlage, "Tunability of superconducting metamaterials," *IEEE Transactions on Applied Superconductivity*, Vol. 17, 918–921, 2007.
19. Gu, J., R. Singh, Z. Tian, W. Cao, Q. Xing, M. He, J. W. Zhang, J. Han, H. T. Chen, and W. Zhang, "Terahertz superconductor metamaterial," *Applied Physics Letters*, Vol. 97, 071102, 2010.
20. Jin, B. B., J. B. Wu, C. H. Zhang, X. Q. Jia, T. Jia, L. Kang, J. Chen, and P. H. Wu, "Enhanced slow light in superconducting electromagnetically induced transparency metamaterials," *Supercond. Sci. Technol.*, Vol. 26, 074004, 2013.
21. Jin, B. B., C. H. Zhang, S. Engelbrecht, A. Pimenov, J. B. Wu, Q. Y. Xu, C. H. Cao, J. Chen, W. W. Xu, L. Kang, and P. H. Wu, "Low loss and magnetic field-tunable superconducting terahertz metamaterial," *Optics Express*, Vol. 18, 17504–17509, 2010.
22. Wu, J. B., B. B. Jin, Y. H. Xue, C. H. Zhang, H. Dai, L. B. Zhang, C. H. Cao, L. Kang, W. W. Xu, J. Chen, and P. H. Wu, "Tuning of superconducting niobium nitride terahertz metamaterials," *Optics Express*, Vol. 19, 12021–12026, 2011.
23. Zhang, C. H., J. B. Wu, B. B. Jin, Z. M. Ji, L. Kang, W. W. Xu, J. Chen, M. Tonouchi, and P. H. Wu, "Low-loss terahertz metamaterial from superconducting niobium nitride films," *Optics Express*, Vol. 20, 42–47, 2012.
24. Zhang, Y. G., J. B. Wu, et al., "Effect of loss and coupling on the resonance of metamaterial: an equivalent circuit approach," *Science China (Information Sciences)*, Vol. 57, 122401, 2014.
25. Prosvirnin, S., S. Zouhdi, et al., "Resonances of closed modes in thin arrays of complex particles," *Advances in Electromagnetics of Complex Media and Metamaterials*, Kluwer Academic Publishers, Netherlands, 281–290, 2003.

26. Tassin, P., L. Zhang, R. Zhao, et al., "Electromagnetically induced transparency and absorption in metamaterials: The radiating two-oscillator model and its experimental confirmation," *Physical Review Letters*, Vol. 109, No. 18, 187401, 2012.
27. Alzar, C. L. G., M. A. G. Martinez, and P. Nussenzeig, "Classical analog of electromagnetically induced transparency," *American Journal of Physics*, Vol. 70, 37, 2002.
28. Zhang, Y. G., J. B. Wu, et al., "Tailoring electromagnetically induced transparency effect of terahertz metamaterials on ultrathin substrate," *Science China (Information Sciences)*, Vol. 59, 042414, 2016.